

Finite source modelling of magmatic unrest in Socorro, New Mexico, and Long Valley, California

Yuri Fialko,^{1,*} Mark Simons¹ and Yakov Khazan²

¹Seismological Laboratory, California Institute of Technology, Pasadena, CA 91125, USA. E-mails: fialko@gps.caltech.edu; simons@caltech.edu

²Department of Tectonophysics, Institute of Geophysics, Kiev, 252680, Ukraine. E-mail: khazan@igph.kiev.ua

Accepted 2001 February 11. Received 2001 February 8; in original form 2000 March 23

SUMMARY

We investigate surface deformation associated with currently active crustal magma bodies in Socorro, New Mexico, and Long Valley, California, USA. We invert available geodetic data from these locations to constrain the overall geometry and dynamics of the inferred deformation sources at depth. Our best-fitting model for the Socorro magma body is a sill with a depth of 19 km, an effective diameter of 70 km and a rate of increase in the excess magma pressure of 0.6 kPa yr^{-1} . We show that the corresponding volumetric inflation rate is $\sim 6 \times 10^{-3} \text{ km}^3 \text{ yr}^{-1}$, which is considerably less than previously suggested. The measured inflation rate of the Socorro magma body may result from a steady influx of magma from a deep source, or a volume increase associated with melting of the magma chamber roof (i.e. crustal anatexis). In the latter case, the most recent major injection of mantle-derived melts into the middle crust beneath Socorro may have occurred within the last several tens to several hundreds of years. The Synthetic Interferometric Aperture Radar (InSAR) data collected in the area of the Long Valley caldera, CA, between June 1996 and July 1998 reveal an intracaldera uplift with a maximum amplitude of $\sim 11 \text{ cm}$ and a volume of $3.5 \times 10^{-2} \text{ km}^3$. Modelling of the InSAR data suggests that the observed deformation might be due to either a sill-like magma body at a depth of $\sim 12 \text{ km}$ or a pluton-like magma body at a depth of $\sim 8 \text{ km}$ beneath the resurgent dome. Assuming that the caldera fill deforms as an isotropic linear elastic solid, a joint inversion of the InSAR data and two-colour laser geodimeter data (which provide independent constraints on horizontal displacements at the surface) suggests that the inferred magma chamber is a steeply dipping prolate spheroid with a depth of 7–9 km and an aspect ratio in excess of 2:1. Our results highlight the need for large radar look angles and multiple look directions in future InSAR missions.

Key words: geodesy, inflation, Long Valley, magma, sill, Socorro.

1 INTRODUCTION

Magma intrusion plays a fundamental role in the formation of the Earth's crust, both oceanic and continental. Our inability to make direct observations of magma emplacement limits our knowledge about the intrusion dynamics to theoretical models, laboratory experiments and field studies of ancient eroded magma bodies (e.g. Pollard & Johnson 1973; Corry 1988; Lister & Kerr 1991). However, when magma intrusion occurs sufficiently rapidly (e.g. on timescales ranging from days to tens of years), and produces sufficiently large deformations of the host rocks, it may lend itself to studies using geodetic

techniques (for a comprehensive review, see Dvorak & Dzurisin 1997). Measurements of crustal deformation induced by magma migration are also important for forecasting local volcanic and seismic hazards.

A prime example of an ongoing crustal intrusion with geodetically documented deformation is the Socorro magma body (New Mexico, USA) (e.g. Sanford & Einarsson 1982). The Socorro magma body is located on the intersection of the Socorro fracture zone and the Rio Grande rift. It is presumably one of the largest currently active magma chambers in the Earth's continental crust. The depth to the intrusion roof, as estimated from the reflection phases of local microearthquakes (Rinehart & Sanford 1981; Balch *et al.* 1997) and seismic reflection surveys (Brown *et al.* 1987), is about 19 km. Interpretation of seismic data suggests that the thickness of the

*Now at: Institute of Geophysics and Planetary Physics, UCSD, La Jolla, CA 92093, USA. E-mail: fialko@radar.ucsd.edu

magma body is of the order of a few hundred metres or less, while the lateral extent is at least 3400 km² (Ake & Sanford 1988; Balch *et al.* 1997). The Socorro magma body is associated with a region of high seismicity, with earthquakes often occurring in swarms (Balch *et al.* 1997), a geoelectric anomaly in the mid-to lower crust (Hermance & Neumann 1991) and a long-term uplift of about 2 mm yr⁻¹ (Reilinger & Oliver 1976; Larsen *et al.* 1986). Geomorphological studies of Holocene terraces in the Socorro area have been interpreted as indicating that this uplift may have continued for the last several tens of thousands of years (Bachman & Mehnert 1978; Ouchi 1983). Larsen *et al.* (1986) employed the results of the finite element modelling of Dieterich & Decker (1975) to simulate vertical displacements measured by levelling surveys in the Socorro area between 1911 and 1981 and concluded that the geodetic data may be explained by magma injection into the seismically imaged Socorro magma body. Because the numerical results of Dieterich & Decker (1975) grossly overestimate vertical displacements due to sill-like magma bodies (Fialko *et al.* 2000 hereafter referred to as Paper I), and because Larsen *et al.* (1986) assumed (rather than solved for) a position of the inflating sill beneath Socorro, we reinterpret the levelling data from Socorro by performing a non-linear inversion of the data using exact solutions for a uniformly pressurized penny-shaped crack (Paper I). We use the results of our inversion to constrain the volumetric inflation rate and speculate on possible causes of the inferred inflation rate of the Socorro magma body.

Another well-studied area of active magmatic deformation is the Long Valley caldera (California, USA) (e.g. Hill *et al.* 1985). The Long Valley caldera is located east of the Sierra Nevada range in Eastern California. It is a large, 32 by 17 km, silicic caldera that formed as the result of an explosive eruption and collapse about 760 kyr ago (Savage *et al.* 1987). The most recent eruption in the Long Valley area occurred several hundred years ago (Sieh & Bursik 1986). The central part of the Long Valley caldera is occupied by a resurgent dome that rises more than 100 m above the caldera floor. The presence of an upper crustal magma reservoir (or several reservoirs) beneath the caldera floor has been inferred from high attenuation (Sanders 1984; Ponko & Sanders 1994) as well as refraction and velocity reduction of seismic waves (Hill *et al.* 1985), geothermal activity and geodetically documented episodes of uplift during the last 30 yr (Savage *et al.* 1987; Langbein *et al.* 1995; Thatcher & Massonnet 1997). The most recent (1997–1998) episode of inflation in Long Valley was imaged in great detail by the European Space Agency Interferometric Synthetic Aperture Radar (InSAR) satellites. Deformation in Long Valley is also monitored by periodic levelling and Global Positioning System (GPS) surveys (Marshall *et al.* 1997) and a frequently surveyed two-colour laser geodimeter network (Langbein *et al.* 1995). These observations make the Long Valley caldera one of the best geodetically monitored volcanic regions in the world. It may therefore be considered as a control case for investigating the robustness of interpretations of geodetic data regarding the position, morphology and dynamics of the inferred magma body (or bodies) at depth. We will use two end-member models, a horizontal circular crack (Paper I) and a finite prolate spheroidal cavity (Yang *et al.* 1988) to model the InSAR and two-colour laser data encompassing the 1997–1998 inflation crisis in Long Valley and we will discuss the implications from our simulations for the geometry of the magma storage region beneath the Long Valley caldera.

2 DEFORMATION IN SOCORRO, NM

2.1 Data and modelling

Fig. 1 shows a schematic map of the Socorro magma body as inferred from early seismic studies (Sanford *et al.* 1973; Rinehart & Sanford 1981). A more recent investigation by Balch *et al.* (1997) suggests that the magma body may have a larger area and a greater extent in the southeast direction. Solid lines in Fig. 1 denote levelling routes occupied in geodetic surveys between 1911 and 1981 (Larsen *et al.* 1986). Vertical displacements observed along these routes are shown in Fig. 2 (open circles). Displacements along the southern part of the N–S levelling route were measured during the 1951–1981 survey, and displacements along the northern part of the N–S route represent measurements between 1911 and 1951 that were extrapolated to the 1951–1981 time period assuming a constant rate of deformation. The western and eastern profiles (see Fig. 2) were surveyed between 1934 and 1979, and 1911 and 1959, respectively. Data for these profiles are also scaled to represent elevation changes during a 30 yr interval between 1951 and 1981 under the assumption that the deformation rate is constant (see Larsen *et al.* 1986, for details). A pronounced feature of the observed deformation is a central uplift of several centimetres that approximately coincides with the seismologically inferred extent of the Socorro magma body. This uplift has been interpreted as an indication of magma injection into a mid-crustal sill beneath Socorro (Reilinger & Oliver 1976; Larsen *et al.* 1986). Another interesting feature apparent in the levelling data is the presence of peripheral subsidence areas (Fig. 2) that have a smaller wavelength but a similar amplitude compared to the uplift anomaly. We note that while the subsidence south of Socorro is inferred from both 1912–1951 and 1951–1981 levelling data, the subsidence around Belen is inferred from the data collected prior to 1951 only (Larsen *et al.* 1986).

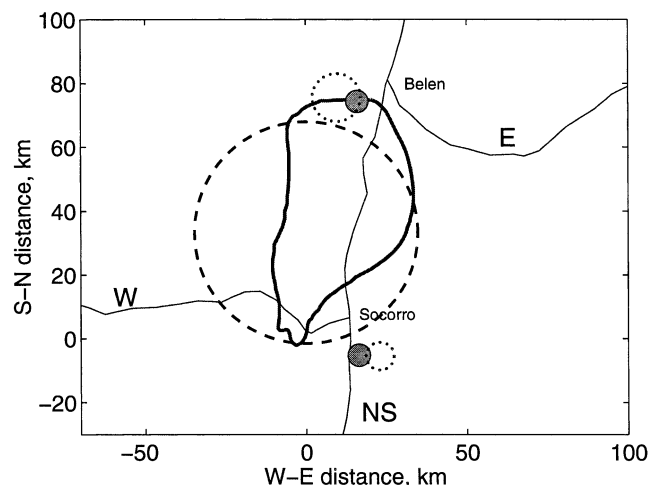


Figure 1. Map of the Socorro magma body as inferred from seismic data (thick irregular line). Thin solid lines are profiles occupied during the 1912–1951 and 1951–1980 levelling surveys. Geographic coordinates of the origin are 34°N, 107°W. Modified from Fig. 11 of Larsen *et al.* (1986). Also shown are the projections of three penny-shaped cracks that provide the best fit to the levelling data: the dashed circle corresponds to an inflating crack at depth of 19.1 km and the dotted circles represent deflating cracks beneath Belen and Socorro (see Table 1). Small solid circles denote the positions of two deflating spherical magma chambers proposed by Larsen *et al.* (1986).

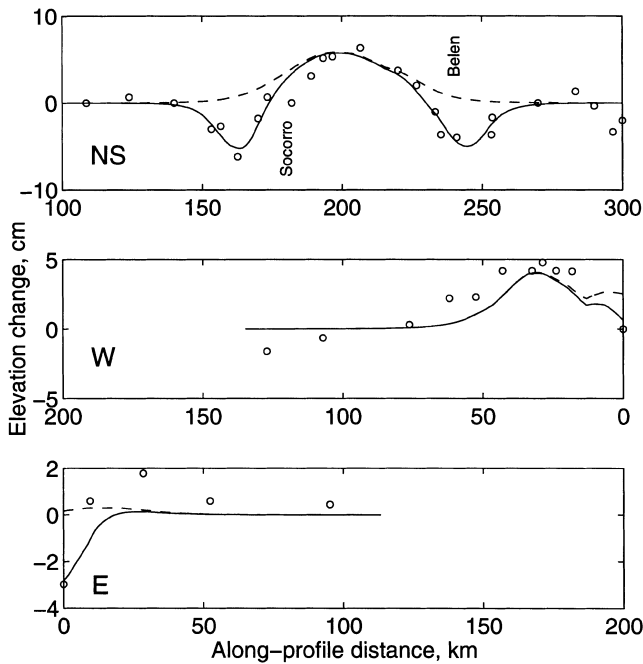


Figure 2. Observed vertical displacements along the north–south (NS), western (W) and eastern (E) levelling profiles (see Fig. 1) are shown as open circles. Data are taken from Figs 12 and 13 of Larsen *et al.* (1986). Solid lines denote predicted deformation for a model of an inflating circular sill at a depth of 19 km and two deflating sills at shallower depths (see Table 1). Dashed line shows predicted deformation due to the inflating sill only.

Larsen *et al.* (1986) used the finite element calculations of Dieterich & Decker (1975) to simulate the observed deformation assuming a model of an inflating sill at a depth of 19 km, and two deflating spherical magma chambers located at the same depth at the sill periphery (filled circles in Fig. 1). Deflating magma chambers were introduced to explain the marginal subsidence areas deduced from the levelling data (Fig. 2). Such an explanation seems to be somewhat *ad hoc*, in particular because it is difficult to justify magma withdrawal from the sill tips towards the sill interiors on physical grounds (e.g. Spence & Sharp 1985; Lister & Kerr 1991). Also, this interpretation implies coincidental appearance of the deflating magma chambers on the levelling routes (Fig. 1). Because the Dieterich & Decker (1975) model used by Larsen *et al.* (1986) has been shown to be inaccurate (Paper I), we perform a non-linear least-squares inversion of the existing levelling data using exact solutions for a uniformly pressurized penny-shaped crack in an elastic half-space. In our simulations we constrain the depth of a mid-crustal inflating sill within the seismologically determined range of 19 ± 0.1 km (Rinehart & Sanford 1981; Balch *et al.* 1997) and impose an upper bound of 70 km on the sill diameter (a characteristic size of the crustal reflector; see Fig. 1). The position of the mid-crustal sill and the excess magma pressure inside the sill are determined using a non-linear least-squares minimization procedure (for details of the inversion algorithm, see Fialko & Simons 2000). To account for the observed peripheral subsidence (see Fig. 1), we introduce two deflating cracks. Positions, depths and sizes of the deflating cracks are free parameters in the inversion. Fig. 2 compares the observed elevation changes along the levelling routes (open circles) to predictions of the best-fitting model (solid lines). Parameters

of the model illustrated in Figs 1 and 2 are listed in Table 1. We also performed an inversion in which no constraints were imposed on the inflating sill dimension. An unconstrained inversion favours a model of a large sill with radius $R \sim 60$ –70 km, which better fits the small-amplitude but broad uplift anomalies apparent along the eastern and western levelling profiles (Figs 1 and 2). Such a large intrusion would be inconsistent with seismic data, and therefore we regard the small uplift anomalies as spurious. The absence of a broad uplift around Socorro is corroborated by the InSAR measurements of deformation for the time period between 1992 and 1999 (Fialko & Simons 2001a). Given the limited spatial coverage of levelling data, the assumption that the size of the inflation source does not exceed the size of the mid-crustal seismic reflector seems to be justified.

Our preferred model (Table 1) consists of an inflating sill of radius ~ 35 km (see dashed circle in Fig. 1), and two deflating sills at a depth of ~ 9 –11 km beneath Belen and Socorro (dotted circles in Fig. 1). The horizontal positions of the deflating sills are similar to those inferred by Larsen *et al.* (1986) for two Mogi sources using a trial-and-error approach. As discussed in Paper I, the levelling data alone do not allow us to distinguish between spheroidal and sill-like sources and make accurate estimates of the source depths. Nonetheless, our simulations indicate that the data fit degrades for deflation sources deeper than ~ 13 km, even if they are represented by point cracks (that is, cracks that are small in size compared to the crack depth). The corresponding ‘upper bound’ depth is less for the Mogi source still, as the latter gives rise to a broader deformation compared to a point crack (see Fig. 4 in Paper I). Thus, provided the inferred ground subsidence is a result of elastic deformation, the levelling data are strongly suggestive of a shallow (i.e. upper crustal) origin of the deflation sources. Because the source depths can effectively trade-off with lateral source dimensions (Paper I), and because the levelling data are too sparse and uncertain to allow a robust inversion, we are unable to put a lower bound on the admissible source depths (that is, the deflation sources might be essentially near surface).

2.2 Origin of uplift: continual magma injection or *in situ* melting?

As demonstrated in Paper I, for sill-like magma bodies one may infer source volume changes by determining the volume of the surface uplift/subsidence. Table 1 gives the volume changes of

Table 1. Source parameters obtained from constrained non-linear inversion.

Parameters	Sources		
	1	2	3
x_0 , km	−0.7	9.1	23.6
y_0 , km	33.1	75.6	−5.5
Depth H , km	19.1	9.1	11.2
Excess magma pressure, $\Delta P/\mu \times 10^5$, Pa	0.1	−11.3	−11.8
Radius R , km	34.7	8.5	6.4
Volume change V , km ³	0.19	−0.17	−0.07

A Poisson’s ratio of 0.25 is used in all calculations.

1: central inflating sill

2: deflating sill near Belen

3: deflating sill near Socorro, see Fig. 1.

the Socorro magma body, as well as the hypothesized deflation sources, deduced from our inversion. Keeping in mind that the results presented in Table 1 correspond to a 30 yr period of deformation between 1951 and 1981, the estimated inflation rate of the Socorro magma body is $\sim 6 \times 10^{-3} \text{ km}^3 \text{ yr}^{-1}$. This value is an order of magnitude less than the inflation rate of $\sim 5 \times 10^{-2} \text{ km}^3 \text{ yr}^{-1}$ inferred by Larsen *et al.* (1986) using the sill model of Dieterich & Decker (1975). Assuming a host rock rigidity of $\mu = 3 \times 10^{10} \text{ Pa}$, we find that the observed uplift rate of a few millimetres per year and a volumetric inflation rate of $\sim 6 \times 10^{-3} \text{ km}^3 \text{ yr}^{-1}$ imply an increase in the excess magma pressure at a rate $\Delta \dot{P} \sim 0.6 \text{ kPa yr}^{-1}$ (see Fig. 3 in Paper I).

A nearly constant inflation rate of several millimetres per year inferred from the geodetic and geomorphic studies in the Socorro area is perhaps surprising, given that geodetic data from other active crustal magma chambers reveal episodic uplift and subsidence on timescales from days to years (see Section 3 below; Savage *et al.* 1987; Dvorak & Dzurisin 1997; Lanari *et al.* 1998). One possibility is that the constant inflation rate in Socorro indicates a continual supply of magma from the mantle source. It has been suggested that the long-term uplift rate of a few millimetres per year and the seismically inferred thickness of the Socorro magma body of $\sim 100 \text{ m}$ (Brocher 1981; Ake & Sanford 1988) may be consistent with the formation of the Socorro sill by a steady-state melt injection over the last several tens of thousands of years (Schlue *et al.* 1996). However, simple thermal arguments indicate that such a scenario is unlikely, as the minimum freezing rate of a 100 m thick (or thinner) sheet intrusion is significantly greater than a few millimetres per year (e.g. Carslaw & Jaeger 1959; Fialko & Rubin 1999). Below we investigate the possibility that the observed uplift in Socorro represents volume changes associated with *in situ* crustal melting. It is well known that heat advected by intrusions of basaltic magmas into the continental crust may be sufficient to give rise to a large-scale melting of the ambient crustal rocks (i.e. anatexis); this melting may continue even after the intruded basalts have completely solidified (e.g. Huppert & Sparks 1988). Because melting of silicate rocks is associated with a volume increase $\gamma = \Delta V/V_0 \sim 10$ per cent, where V_0 is the initial volume of solid rock and ΔV is the volume increment upon fusion (e.g. McBirney 1993), the observed deformation in Socorro might be explained by the generation of anatectic melts at a rate of $\dot{V}/\gamma \sim O(0.1 \text{ km}^3 \text{ yr}^{-1})$, where \dot{V} is the geodetically measured inflation rate. Dividing the inferred rate of melt generation by the sill area πR^2 (see Table 1), and assuming that melting occurs in the intrusion roof, we obtain a roof melting rate of the order of centimetres per year. A theoretical estimate of the rate of melting of the intrusion roof can be obtained by balancing the heat loss from the magma chamber with the specific and latent heat required to fuse the ambient crustal rocks. Assuming that the heat loss from the intrusion is dominated by conduction, a steady-state melting rate \dot{m} is given by [e.g. Huppert & Sparks (1988); see their eq. 6]

$$\dot{m} = \frac{k \Delta T_m}{d \rho_s (c \Delta T_0 + L)}, \quad (1)$$

where k is the thermal conductivity of melt, d is the average thickness of the melt layer, ρ_s , c and L are the density, specific heat and latent heat of the ambient rocks, respectively, ΔT_m is the temperature difference between the rock solidus temperature and the average magma temperature within the intrusion and

ΔT_0 is the host rock undercooling (the difference between the initial rock temperature and the solidus). For a geothermal gradient of 30 K km^{-1} and a melting temperature of the crustal rocks of 1100 K , the host rock undercooling at a depth of 19 km is $\Delta T_0 \sim 250 \text{ K}$. Using typical values of thermo-physical parameters for silicate rocks, $\rho_s = 2.8 \times 10^3 \text{ kg m}^{-3}$, $c = 10^3 \text{ J kg}^{-1} \text{ K}^{-1}$ and $L = 4 \times 10^5 \text{ J kg}^{-1}$ (e.g. McBirney 1993) and a sill thickness of 100 m (Brocher 1981; Ake & Sanford 1988) and assuming $\Delta T_m \sim 100 \text{ K}$ (Huppert & Sparks 1988), from eq. (1) we deduce a melting rate of the intrusion roof of $\dot{m} \sim O(\text{cm yr}^{-1})$. The melting rate is likely to be higher in the presence of convection within the fused layer. Note, however, that the thermally induced inflation rate may be less than $\gamma \dot{m}$ because melting of the magma chamber roof may be accompanied by cooling and crystallization of the fused layer, as well as the mafic sill. For a sill of thickness H_i , surface displacements U_z due to thermodynamic effects may be calculated as follows:

$$U_z(t) = H_h(t)(1 - \alpha_h(t))\gamma_h - H_i \alpha_i(t)\gamma_i, \quad (2)$$

where t is the time since sill emplacement, H_h is the thickness of the fused layer, α is the volume fraction of crystallized melt and indexes h and i correspond to the fused host rock and intruded mafic melt, respectively. All time-dependent parameters on the right-hand side of eq. (2) may be found by solving a Stefan-type boundary value problem of heat transfer and phase transitions due to sill intrusion. The corresponding problem has been solved by Huppert & Sparks (1988) using empirical relationships between magma temperature, crystal content and viscosity for a range of initial sill thicknesses H_i (e.g. see their Fig. 4). Taking the results of Huppert & Sparks at face value, eq. (2) predicts negative U_z (i.e. subsidence) immediately following sill emplacement due to crystallization of the intruded mafic magma. However, the direction of vertical displacements reverses, and uplift commences when crystallization of the mafic sill is nearly complete, but the thickness of the fused layer H_h continues to increase. The rate and duration of the thermally induced uplift depends on the initial thickness of the mafic sill H_i ; for H_i varying from 100 to 500 m , the duration of uplift is of the order of 10 – 10^2 yr , and the uplift rates are of the order of 10^{-3} – $10^{-2} \text{ m yr}^{-1}$. The calculations of Huppert & Sparks assume that the emplacement of a mafic sill occurs instantaneously or on a timescale that is small compared to the solidification timescale. In the case of intrusion formation by gradual or episodic magma replenishment on timescales comparable to or greater than the freezing timescale, the generation of anatectic melts is less robust.

Dimensional estimates confirmed by detailed numerical experiments indicate that a 100 m thick intrusion will freeze on a timescale of 100 yr if the heat lost from the magma to the host rocks is by conduction alone (e.g. Fialko & Rubin 1998; Fialko & Rubin 1999), and even sooner in the presence of convection (Huppert & Sparks 1988). It follows that either the Socorro magma body is much younger than the geomorphologically inferred uplift (estimated uplift age $\sim 5 \times 10^4 \text{ yr}$) (Bachman & Mehnert 1978; Ouchi 1983), or the total uplift amplitude ($\sim 100 \text{ m}$) is a small fraction of the intrusion thickness. A large intrusion thickness suggested by thermal arguments might be reconciled with the (much smaller) uplift inferred from geomorphological data if elastic stresses due to magma injection are partially relaxed by some mechanism (e.g. viscoelastic deformation of the host rocks). Irrespective of the age of the Socorro magma body, our results demonstrate that the geodetically

documented uplift rates of a few millimetres per year may be explained by (and, in fact, are the expected consequence of) crustal anatexis due to the intrusion of mafic melts into the middle crust beneath the Rio Grande Rift. If melt supply is episodic, the thermally induced uplift following magma injection is expected to occur at a rate that scales as the inverse square root of time [that is, characteristic of a diffusive process, e.g. Carslaw & Jaeger (1959)]. While the available levelling data are too infrequent to determine the details of the uplift history in the Socorro area, an apparent decrease in the uplift rate and seismicity between the periods 1911–1951 and 1951–1981 has been reported (Larsen *et al.* 1986). This decrease may indicate either a decline in magma supply or magma cooling and concomitant deceleration of roof melting. In the latter case, the most recent major injection of basaltic melts that might have caused the hypothesized melting of the host rocks may have taken place several tens to several hundreds of years ago. Provided that seismicity in the Socorro area is related to deformation due to inflation of the Socorro magma body (Ake & Sanford 1988; Balch *et al.* 1997), a series of moderate (up to magnitude 6) earthquakes that occurred in the vicinity of Socorro in 1906–1907 (Reid 1911) might be a manifestation of such an injection episode (Guterman *et al.* 1997; Fialko 2001). InSAR observations in the Socorro area indicate that the uplift continued at a rate of 2–4 mm yr⁻¹ between 1992 and 1999 (Fialko & Simons 2001a).

While the central uplift near Socorro seems to be well explained by the inflation of the mid-crustal magma body, the origin of peripheral subsidence areas deduced from the levelling data (Fig. 2) is not well understood. Similar to the above arguments, one might suggest that the areas of subsidence represent crystallization of magma in shallow intrusions. Using estimates of deflation volumes for crack-like sources from our inversion (Table 1), we infer that the observed subsidence might be explained by crystallization of 1.7 and 0.7 km³ of magma over a 30 yr period in the upper crust beneath Belen and Socorro, respectively. Shallow magma intrusions at depths of between 5 and 10 km have been inferred from microearthquake studies (Sanford 1983). Alternatively, the flanking subsidence may be a result of inelastic deformation of the crust in response to magma withdrawal from a deep source. Guterman *et al.* (1996) studied large-scale inelastic deformation associated with a ‘deflating mantle source–inflating crustal sill’ system using centrifuged physical analogue models of Mohr–Coulomb materials (such as various mixtures of clay, graphite and chalk powder). Such models produced a central uplift as well as the peripheral troughs due to deflation of a deep source feeding the crustal sill. In the experiments of Guterman *et al.* (1996), the bulk of the subsidence due to fluid withdrawal from a deep source was accommodated along two inward-dipping shear zones, one extending from a shallow sill towards the surface with a reverse sense of motion and the other extending from a deep source towards the surface with a normal sense of motion (see Fig. 6 of Guterman *et al.* 1996). Guterman *et al.* (1996) inferred that the best fit to the geodetic data of Larsen *et al.* (1986) is provided by a model in which a deep source has a depth of about 50 km and a characteristic lateral dimension of ~140 km. However, it is unclear whether the (purely brittle) physical analogue models of Guterman *et al.* (1996) adequately describe deformation in the lower crust, where significant viscoelastic relaxation may occur on timescales comparable to the intervals between the levelling data acquisitions (i.e. tens of years).

We note that an apparent correlation between the regions of subsidence and populated areas (Figs 1 and 2) suggests that shallow man-induced processes (such as water pumping) may be suspected as a cause of deflation. Larsen *et al.* (1986) argued that water withdrawal from the ground is not a likely cause of the observed subsidence because water pumping in the Belen area did not appreciably affect the local water table (Titus 1963), and because only small amounts of groundwater were withdrawn in the Socorro area. A similar area of subsidence at the northern end of the N–S profile (Fig. 2) has, however, been attributed to water pumping near Albuquerque (Reilinger *et al.* 1980). Note that the spherical deflation sources in the middle crust beneath Belen and Socorro (i.e. the preferred model of Larsen *et al.* 1986) would imply a surface contraction in these areas giving rise to a strain rate of the order of (subsidence rate)/(source depth). That is, for a subsidence rate of several millimetres per year and a source depth of 19 km, the corresponding strain rate is $O(10^{-7} \text{ yr}^{-1})$. While horizontal strain rates of this magnitude were recorded in the vicinity of Socorro during a 1972–1984 trilateration survey (Savage *et al.* 1985), the inferred strains revealed no systematic temporal pattern, and in fact changed their sign during the period of observation. The absence of a systematic strain accumulation in the trilateration data of Savage *et al.* (1985) argues against volume changes in the middle crust below the Rio Grande rift. At the same time, the trilateration data do not exclude the possibility of shallow (several kilometres or less) and ‘distributed’ deflation sources that do not produce measurable horizontal displacements. Further progress in understanding the nature of the inferred subsidence areas on the periphery of the uplift due to the Socorro magma body requires more detailed mapping of surface deformation (both vertical and horizontal) around the hypothesized deflation sources.

3 DEFORMATION IN LONG VALLEY, CA

Long Valley caldera in eastern California has experienced several periods of magmatic unrest during the last several decades (Savage *et al.* 1987; Dvorak & Dzurisin 1997). The most recent episode of inflation and uplift of the resurgent dome within the caldera occurred in 1997–1998. Since 1992, the area of Long Valley has been repeatedly imaged by the European Space Agency satellites ERS 1 and 2. We analyse crustal deformation in Long Valley during the 1997–1998 inflation crisis using the Interferometric Synthetic Aperture Radar (InSAR) data collected by the ERS satellites. The ERS radar data have been processed using the JPL/Caltech repeat orbit interferometry package ROI_PAC. Fig. 3 shows an unwrapped flattened interferogram from a descending orbit (track 485, frame 2840), with radar acquisition dates of 1996 June 6 and 1998 July 12. The effects of topography are removed from the interferometric image using a mosaic of the 7.5′ United States Geological Survey (USGS) digital elevation maps (DEM). The interferogram shown in Fig. 3 has a small perpendicular baseline (16 m), indicating that it is relatively insensitive to DEM errors. The InSAR data reveal a domal uplift of the Earth’s surface within the Long Valley caldera, with a maximum displacement of ~10 cm in the satellite line of sight (LOS) direction. Because the ERS satellites have a small look angle (about 20° from the vertical in the area of study), the line of sight displacements shown in Fig. 3 probably indicate predominantly vertical motion of the

ground [projections of a unit vector towards the satellite onto the (east, north, up) axes are (0.38, −0.09, 0.92), respectively]. Given that the observed deformation has a characteristic ‘bull’s eye’ pattern (Fig. 3), it is reasonable to expect that the deformation source is nearly axisymmetric. To obtain further insight into the morphology of the inferred magma body beneath the Long Valley caldera, we invert the InSAR data for two ‘end-member’ source geometries—a sill (Paper I) and a prolate finite spheroid of arbitrary orientation (Yang *et al.* 1988). Because details of the source geometry cannot be resolved with only one component of the displacement field (e.g. Dieterich & Decker 1975), we include in our analysis the two-colour laser geodimeter data (unpublished data courtesy of J. Langbein, USGS, 2000). The two-colour laser data provide accurate measurements of baseline changes within a trilateration network spanning the resurgent dome (for details see e.g. Langbein *et al.* 1995). Fig. 4 shows the results of our calculations. As one can see from Fig. 4, both models are able to fit the InSAR data reasonably well. Table 2 summarizes the parameters of the best-fitting sill and prolate spheroid models. Source geometries similar to those reported in Table 2 are also obtained in the inversion using a stack of four interferograms acquired between 1996 and 1999 (stacking of long-term interferograms may reduce atmospheric effects and increase signal-to-noise ratio). The InSAR measurements are intrinsically relative, in that the radar phase differences correspond to the ‘true’ LOS displacements plus an unknown (generally non-zero) constant. Therefore, in our modelling we include a constant shift in the LOS data as a free parameter. We also allow for a long-wavelength linear trend in the LOS data to compensate for possible errors in satellite orbits and artefacts due to flattening of the interferograms during data processing. The long-wavelength ramp coefficients are determined as part of the inversion. The best-fitting sill model (Figs 4a–c) suggests that the magma body has a depth of ~ 12 km and a radius of ~ 1.6 km. Because the inferred sill dimension is a small fraction of the sill depth, the deformation source is essentially a ‘point crack’. For a point crack, the maximum amplitude of the surface uplift, U_z^{\max} , is given by (Sun 1969; Fialko *et al.* 2001)

$$U_z^{\max} = \frac{4}{\pi} \frac{1-\nu}{\mu} \Delta P \frac{R^3}{H^2}, \quad (3)$$

where ν is the Poisson’s ratio, μ is the shear modulus, ΔP is the excess magma pressure, and R and H are the sill radius and depth, respectively. Note that while the sill depth is constrained by the horizontal extent of the surface uplift, the uplift amplitude depends on the product $R^3 \Delta P / \mu$. Therefore, the excess magma pressure and the source size cannot be determined

independently from geodetic data, as in the case of the Mogi source (e.g. McTigue 1987). Assuming a shear modulus of the host rocks of 10 GPa, our results suggest the excess magma pressure $\Delta P \sim 39$ MPa for a sill with radius $R = 1.6$ km (Table 2). This excess magma pressure is perhaps too high, given that the rock tensile strength is of the order of 10 MPa. For a sill that is a factor of two larger, $R = 3.2$ km, the inferred excess magma pressure is a factor of eight less, $\Delta P \sim 5$ MPa (see eq. 3), which is a more reasonable value.

Simulations using a prolate source suggest that the deformation source may be approximated by a steeply dipping spheroid with a depth of ~ 7 km, major and minor axes of 4.2 and 1.8 km and an increase in the excess pressure of 8 MPa between the summers of 1996 and 1998 (Table 2). The spheroid dimensions may represent an ‘aureole’ of inelastically yielding rocks surrounding the hypothesized magma chamber, and not necessarily the magma chamber itself (Davis 1986). By using the F test with a 95 per cent confidence level, we estimate source location errors of the order of 1 km for both sill and prolate spheroid models.

While the prolate spheroid model is characterized by horizontal displacements that are almost a factor of two larger than those due to a sill, the results shown in Fig. 4 illustrate that the InSAR data alone are unlikely to discriminate between different models of deformation and resolve intrinsic trade-offs between the magma chamber shape and the chamber depth, as the LOS displacements are mostly sensitive to the vertical component of deformation (Paper I). The sensitivity of InSAR measurements to horizontal displacements can be enhanced, for example by increasing the look angle of a satellite radar and by using interferograms from different lines of sight (for example, ascending and descending orbits and multiple radar look directions). Unfortunately, no ascending InSAR data are available for Long Valley for the time period between 1996 and 1998. The ability to resolve both vertical and horizontal components of deformation should be a major consideration in the design of future InSAR missions.

The data from the two-colour geodimeter network operated in Long Valley by the USGS provide important constraints on the morphology of the hypothesized magma body. Fig. 5 shows changes in the baseline lengths measured with respect to the central monument CASA (see Langbein *et al.* 1995, for details), along with predictions of the best-fitting models (Fig. 4 and Table 2). As one can see in Fig. 5, the prolate spheroid model on average provides a better fit to the two-colour laser data. This result is in a general agreement with the study of Langbein *et al.* (1995), who were able to explain the levelling and two-colour data for a period of deformation between 1988 and 1992 using a vertically elongated pressure source at a depth of 7 km. While Langbein *et al.* (1995) argued in favour of a model consisting of two inflation sources, a shallow source at 5.5 km depth beneath the resurgent dome and a deeper source at depths between 10 and 20 km beneath the south moat of the caldera, our results do not lend support to such an interpretation. Although decreases in the source depth do improve the model fit to the two-colour data somewhat, a shallow inflation source at a depth of 5.5 km significantly degrades the fit to the InSAR data. Because the use of elastic half-space models may underestimate horizontal displacements at the Earth surface, as discussed below, fitting of the two-colour data at the expense of a systematic misfit to the InSAR data is likely to bias the solution towards shallow depths and large aspect ratios.

Table 2. Source parameters obtained from the inversion.

Parameters	Sill	Prolate spheroid
x_0 , km	2.3	1.0
y_0 , km	2.2	3.0
Depth z_0 , km	12.1	7.2
Excess magma pressure, $\Delta P / \mu \times 10^5$, Pa	387	80
Major axis a , km	1.6	4.2
Minor axis b , km		1.8
Strike of the major axis, ϕ_a , °		20
Plunge of the major axis, θ_a , °		97

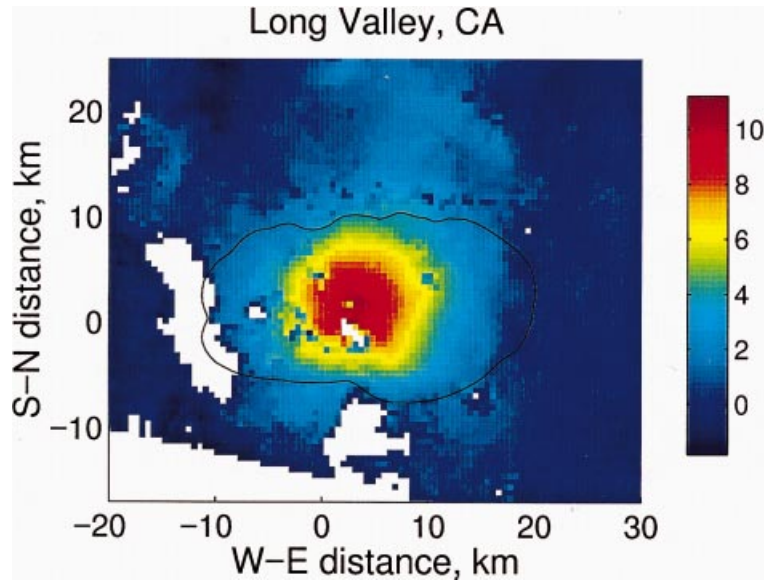


Figure 3. Radar interferogram of Long Valley, eastern California. Colours denote relative displacements of the Earth's surface in the satellite line of sight direction in centimetres (displacements toward the satellite are positive). Geographic coordinates of the origin are $37^{\circ}40'N$, $118^{\circ}55'W$. Black line denotes the boundary of the Long Valley caldera. Areas outside the radar scene, as well as the missing interferometric data (for example, due to decorrelation and radar lay-overs due to steep topography), are shown in white.

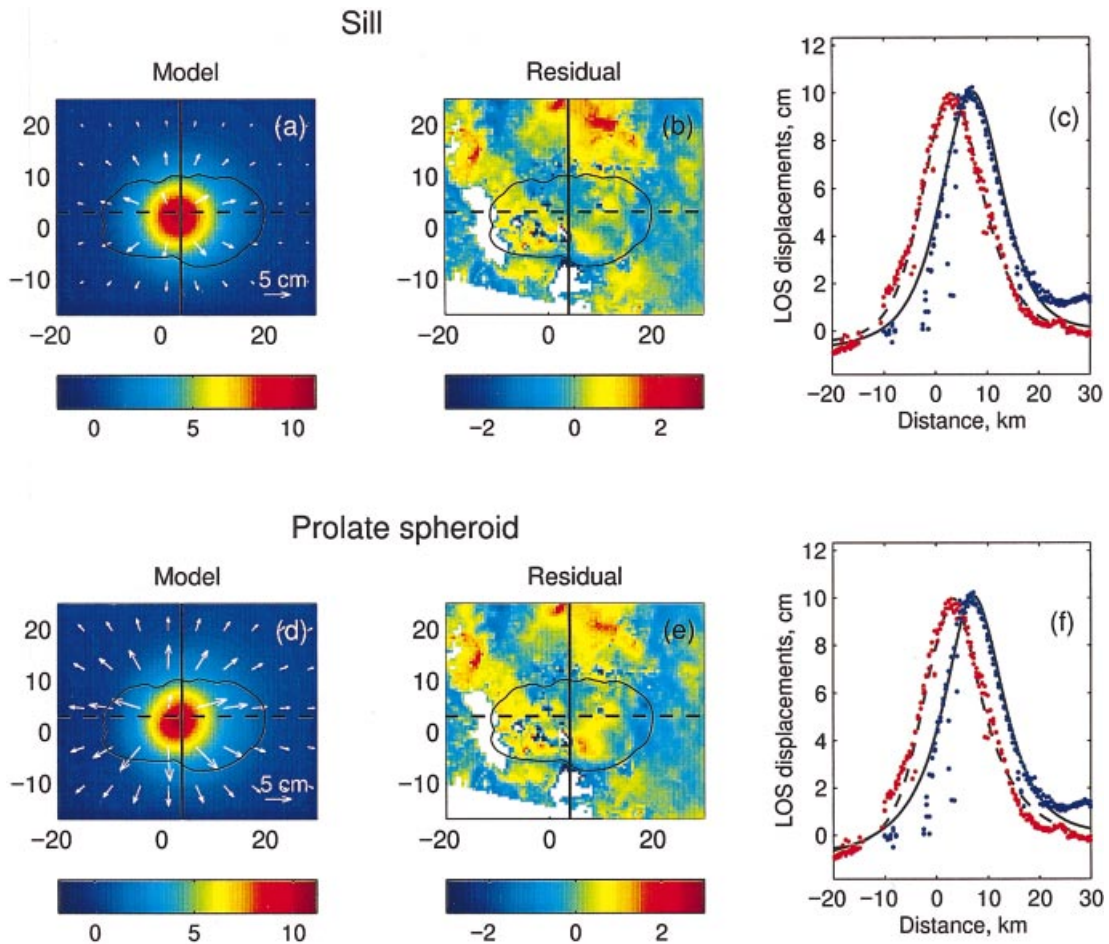


Figure 4. Results of the inversion of the InSAR and two-colour laser geodimeter data from Long Valley, CA, using sill (a–c) and prolate spheroid (d–f) models (see Table 2 for the corresponding source parameters). (a), (d) Modelled LOS displacements. Arrows denote predicted horizontal displacements at the Earth's surface. (b), (e) Residual LOS displacements after subtracting the model from the data (Fig. 3). (c), (f) S–N (blue, solid line) and W–E (red, dashed line) profiles across the resurgent dome. Dots are observed and lines are calculated LOS displacements along the profiles shown in (a) and (d).

and overall geometry of the upper crustal magma reservoir may be difficult without *a priori* knowledge of the mechanical properties (in particular, anisotropy and anelasticity) of the host rocks.

ACKNOWLEDGMENTS

We thank Alan Beck, Paul Davis and an anonymous reviewer for thoughtful comments that helped to improve this manuscript. This work was supported by NSF grant EAR-9980664. The ERS SAR imagery was acquired under the research user category from Eurimage, Italy. The data and modelling results presented in this paper are available from the authors. Seismological Laboratory contribution 8708.

REFERENCES

- Ake, J.P. & Sanford, A.R., 1988. New evidence for the existence and internal structure of a thin layer of magma at mid-crustal depths near Socorro, New Mexico, *Bull. seism. Soc. Am.*, **78**, 1335–1359.
- Bachman, G.O. & Mehnert, H.H., 1978. New K-Ar dates and the late Pliocene to Holocene geomorphic history of the central Rio Grande region, New Mexico, *Geol. Soc. Am. Bull.*, **89**, 283–292.
- Balch, R.S., Hartse, H.E., Sanford, A.R. & Lin, K., 1997. A new map of the geographic extent of the Socorro magma body, *Bull. seism. Soc. Am.*, **87**, 174–182.
- Brocher, T.M., 1981. Geometry and physical properties of the Socorro, New Mexico, magma bodies, *J. geophys. Res.*, **86**, 9420–9432.
- Brown, L.D. *et al.*, 1987. COCORP: New perspectives on the deep crust, *Geophys. J. R. astr. Soc.*, **89**, 47–54.
- Carslaw, H.S. & Jaeger, J.C., 1959. *Conduction of Heat in Solids*, Oxford University Press, New York.
- Corry, C.E., 1988. Laccoliths: mechanism of emplacement and growth, *Geol. Soc. Am. Spec. Pap.*, **220**.
- Davis, P.M., 1986. Surface deformation due to inflation of an arbitrarily oriented triaxial ellipsoidal cavity in an elastic half-space, with reference to Kilauea Volcano, Hawaii, *J. geophys. Res.*, **91**, 7429–7438.
- Dieterich, J. & Decker, R., 1975. Finite element modeling of surface deformation associated with volcanism, *J. geophys. Res.*, **80**, 4094–4102.
- Dreger, D., Tkalčić, H. & Johnston, M., 2000. Dilational processes accompanying earthquakes in the Long Valley caldera, *Science*, **288**, 122–125.
- Dvorak, J. & Dzurisin, D., 1997. Volcano geodesy: the search for magma reservoirs and the formation of eruptive vents, *Rev. Geophys.*, **35**, 343–384.
- Fialko, Y., 2001. Origin of near-axis faulting and volcanism at the fast spreading mid-ocean ridges, *Earth planet. Sci. Lett.*, in press.
- Fialko, Y.A. & Rubin, A.M., 1998. Thermodynamics of lateral dike propagation: implications for crustal accretion at slow-spreading mid-ocean ridges, *J. geophys. Res.*, **103**, 2501–2514.
- Fialko, Y.A. & Rubin, A.M., 1999. Thermal and mechanical aspects of magma emplacement in giant dike swarms, *J. geophys. Res.*, **104**, 23 033–23 049.
- Fialko, Y. & Simons, M., 2000. Deformation and seismicity in the Coso geothermal area, Inyo County, California: observations and modeling using satellite radar interferometry, *J. geophys. Res.*, **105**, 21 781–21 793.
- Fialko, Y. & Simons, M., 2001a. On-going inflation of the Socorro magma body, New Mexico, as imaged by the Interferometric Synthetic Aperture Radar, *Geophys. Res. Lett.*, in press.
- Fialko, Y. & Simons, M., 2001b. Complete (3-D) surface displacement field due to the 1999 M7.1 Hector Mine earthquake, southern California, from space geodetic observations, *Geophys. Res. Lett.*, submitted.
- Fialko, Y., Khazan, Y. & Simons, M., 2000. Deformation due to a pressurized horizontal circular crack in an elastic half-space, with applications to volcano geodesy, *Geophys. J. Int.*, **146**, 181–190 (this issue).
- Guterman, V.G., Fialko, Y.A. & Khazan, Y.M., 1996. Dome structures over sill-like crustal structures: a numerical model of preseismic uplift. 1. *Geophys. J.*, **16**, 209–226. (English transl.).
- Guterman, V.G., Fialko, Y.A. & Khazan, Y.M., 1997. Dome structures over sill-like crustal structures: a numerical model of preseismic uplift. 2. *Geophys. J.*, **16**, 543–554. (English transl.).
- Hermance, J.F. & Neumann, G.A., 1991. The Rio Grande rift: new electromagnetic constraints on the Socorro magma body, *Phys. Earth planet. Sci.*, **66**, 101–117.
- Hill, D.P., Bailey, R.A. & Ryall, A.S., 1985. Active tectonic and magmatic processes beneath Long Valley caldera, Eastern California; an overview, *J. geophys. Res.*, **90**, 11 111–11 120.
- Huppert, H.E. & Sparks, R.S.J., 1988. The generation of granitic magmas by intrusion of basalt into continental crust, *J. Petrol.*, **29**, 599–624.
- Lanari, R., Lundgren, P. & Sansosti, E., 1998. Dynamic deformation of Etna volcano observed by satellite radar interferometry, *Geophys. Res. Lett.*, **25**, 1541–1544.
- Langbein, J., Hill, D., Parker, T. & Wilkinson, S., 1995. Shallow and peripheral volcanic sources of inflation revealed by modeling two-color geodimeter and leveling data from Long Valley caldera, California, 1988–1992, *J. geophys. Res.*, **100**, 12 487–12 495.
- Larsen, S., Reilinger, R. & Brown, L., 1986. Evidence of ongoing crustal deformation related to magmatic activity near Socorro, New Mexico, *J. geophys. Res.*, **91**, 6283–6293.
- Lister, J.R. & Kerr, R.C., 1991. Fluid-mechanical models of crack propagation and their application to magma transport in dykes, *J. geophys. Res.*, **96**, 10 049–10 077.
- Marshall, G., Langbein, J., Stein, R., Lisowski, M. & Svarc, J., 1997. Inflation of Long Valley caldera, California, Basin and Range strain, and possible Mono Craters dike inflation from 1990–1994 GPS surveys, *Geophys. Res. Lett.*, **24**, 1003–1006.
- McBirney, A., 1993. *Igneous Petrology*, 2nd edn, Jones & Bartlett, Boston, MA.
- McTigue, D.F., 1987. Elastic stress and deformation near a finite spherical magma body: resolution of the point source paradox, *J. geophys. Res.*, **92**, 12 931–12 940.
- Ouchi, S., 1983. Effects of uplift on the Rio Grande over the Socorro magma body, New Mexico, *Field Conf. Guidebook N. M. Geol. Soc.*, **34**, 54–56.
- Peltzer, G., Crampe, F. & King, G., 1998. Evidence of nonlinear elasticity of the crust from the M_w 7.6 Manyi (Tibet) earthquake, *Science*, **286**, 272–276.
- Pollard, D.D. & Johnson, A.M., 1973. Mechanics of growth of some laccolithic intrusions in the Henry Mountains, Utah, I; field observations, Gilbert's model, physical properties and flow of the magma, *Tectonophysics*, **18**, 261–309.
- Ponko, S.C. & Sanders, C.O., 1994. Inversion of P and S wave attenuation structure, Long Valley, California, *J. geophys. Res.*, **99**, 2619–2635.
- Reid, H.F., 1911. Remarkable earthquakes in central New Mexico in 1906 and 1907, *Bull. seism. Soc. Am.*, **1**, 10–16.
- Reilinger, R.E. & Oliver, J.E., 1976. Modern uplift associated with a proposed magma body in the vicinity of Socorro, New Mexico, *Geology*, **4**, 583–586.
- Reilinger, R.E., Oliver, J.E., Brown, L.D., Sanford, A.R. & Balazs, E.I., 1980. New measurements of crustal doming over the Socorro magma body, *Geology*, **8**, 291–295.
- Rinehart, E. & Sanford, A., 1981. Upper crustal structure of the Rio Grande rift near Socorro, New Mexico, from inversion of microearthquake S-wave reflections, *Bull. seism. Soc. Am.*, **71**, 437–450.
- Rubin, A.M., 1992. Dike-induced faulting and graben subsidence in volcanic rift zones, *J. geophys. Res.*, **97**, 1839–1858.

- Sanders, C.O., 1984. Location and configuration of magma bodies beneath Long Valley, California, determined from anomalous earthquake signals, *J. geophys. Res.*, **89**, 8287–8302.
- Sanford, A.R., 1983. Magma bodies in the Rio Grande rift in central New Mexico, *Field Conf. Guidebook N. M. Geol. Soc.*, **34**, 123–125.
- Sanford, A.R. & Einarsson, P., 1982. Magma chambers, in *Continental and Oceanic Rifts*, pp. 147–168, ed. Palmason, G., AGU, Washington, DC.
- Sanford, A.R., Alptekin, O.S. & Topozada, T.R., 1973. Use of reflection phases on microearthquake seismograms to map an unusual discontinuity beneath the Rio Grande rift, *Bull. seism. Soc. Am.*, **63**, 2021–2034.
- Savage, J.C., Lisowski, M. & Prescott, W.H., 1985. Strain accumulation in the Rocky Mountain states, *J. geophys. Res.*, **90**, 310–320.
- Savage, J.C., Cockerham, R.S., Estrem, J.E. & Moore, L.R., 1987. Deformation near the Long Valley caldera, eastern California, 1982–1986, *J. geophys. Res.*, **92**, 2721–2746.
- Schlue, J., Aster, R. & Meyer, R., 1996. A lower crustal extension to a midcrustal magma body in the Rio Grande Rift, New Mexico, *J. geophys. Res.*, **101**, 25 283–25 291.
- Sieh, K. & Bursik, M., 1986. Most recent eruption of the Mono craters, eastern central California, *J. geophys. Res.*, **91**, 2539–2571.
- Spence, D.A. & Sharp, P., 1985. Self-similar solutions for elastodynamic cavity flow, *Proc. R. Soc. Lond.*, **A400**, 289–313.
- Sun, R.J., 1969. Theoretical size of hydraulically induced horizontal fractures and corresponding surface uplift in an idealized medium, *J. geophys. Res.*, **74**, 5995–6011.
- Thatcher, W. & Massonnet, D., 1997. Crustal deformation at Long Valley Caldera, eastern California, 1992–1996 inferred from satellite radar interferometry, *Geophys. Res. Lett.*, **24**, 2519–2522.
- Titus, F.B., 1963. Geology and ground-water conditions in eastern Valencia County, New Mexico, *N. M. Bur. Mines Mineral. Resource Ground Water Rept*, **7**.
- Yang, X.-M., Davis, P.M. & Dieterich, J.H., 1988. Deformation from inflation of a dipping finite prolate spheroid in an elastic half-space as a model for volcanic stressing, *J. geophys. Res.*, **93**, 4249–4257.